Accepted by Astrophysical Journal Letters
Preprint typeset using LaTeX style emulateapj v. 6/22/04

arXiv:astro-ph/0511581v1 18 Nov 2005

# THE EVOLUTION OF REST-FRAME $K$-BAND PROPERTIES OF EARLY-TYPE GALAXIES FROM $Z = 1$ TO THE PRESENT[1,2,3]

A. van der Wel[4], M. Franx[4], P.G. van Dokkum[5], J. Huang[6], H.-W. Rix[7], and G.D. Illingworth[8]

*Accepted by Astrophysical Journal Letters*

## ABSTRACT

We measure the evolution of the rest-frame $K$-band Fundamental Plane from $z = 1$ to the present by using IRAC imaging of a sample of early-type galaxies in the Chandra Deep Field-South at $z \sim 1$ with accurately measured dynamical masses. We find that $M/L_K$ evolves as $\Delta \ln (M/L_K) = (-1.18 \pm 0.10)z$, which is slower than in the $B$-band ($\Delta \ln (M/L_B) = (-1.46 \pm 0.09)z$). In the $B$-band the evolution has been demonstrated to be strongly mass dependent. In the $K$-band we find a weaker trend: galaxies more massive than $M = 2 \times 10^{11} M_\odot$ evolve as $\Delta \ln (M/L_K) = (-1.01 \pm 0.16)z$; less massive galaxies evolve as $\Delta \ln (M/L_K) = (-1.27 \pm 0.11)z$. As expected from stellar population models the evolution in $M/L_K$ is slower than the evolution in $M/L_B$. However, when we make a quantitative comparison, we find that the single burst Bruzual-Charlot models do not fit the results well, unless large dust opacities are allowed at $z = 1$. Models with a flat IMF fit better, Maraston models with a different treatment of AGB stars fit best. These results show that the interpretation of rest-frame near-IR photometry is severely hampered by model uncertainties and therefore that the determination of galaxy masses from rest-frame near-IR photometry may be harder than was thought before.

*Subject headings:* cosmology: observations—galaxies: evolution—galaxies: formation

## 1. INTRODUCTION

The formation and evolution of early-type galaxies (hereafter, E/S0s) has been a major subject of research during the past decades. Both theoretical and empirical studies indicate that the stellar mass density of the ETG population has increased by at least a factor of two between $z = 1$ and the present day (Kauffmann & Charlot 1998; Bell et al. 2004; Faber et al. 2005) At the same time, studies at $z \sim 1$ show that massive E/S0s were already several *Gyr* old at that epoch (van Dokkum & Stanford 2003; Holden et al. 2005; Treu et al. 2005; van der Wel et al. 2005). It is an intriguing puzzle to explain these seemingly contradictory results in one picture describing early-type galaxy formation.

These results hinge on determining galaxy masses, which remains very hard to do at high redshift. Typically, mass estimates for high-$z$ galaxies are obtained by comparing their photometric properties with stellar population models in order to infer a mass-to-light ratio ($M/L$) (see, e.g., Bell et al. 2003; Bundy et al. 2005; Shapley et al. 2005). Such SED-fitting methods are intrinsically uncertain, and dynamical mass calibrations are needed to overcome the large uncertainty in the low mass end of the initial mass function (IMF), dark matter content, and, most importantly, to verify the validity of stellar population models. A more quantitative approach is to use the Fundamental Plane (FP, Djorgovski & Davis 1987; Dressler et al. 1987) to directly measure the evolution of $M/L$ at rest-frame optical wavelengths out to $z = 1.3$ (van Dokkum & Franx 1996; van Dokkum et al. 1998; Kelson et al. 2000; Treu et al. 2001; van Dokkum et al. 2001; Treu et al. 2002; van Dokkum & Stanford 2003; van Dokkum & Ellis 2003; Gebhardt et al. 2003; van der Wel et al. 2004; Wuyts et al. 2004; Holden et al. 2005; Treu et al. 2005; van der Wel et al. 2005).

Although the measurement of the evolution of $M/L$ itself is model independent, the inferred age and formation redshift are sensitive to the choice of the parameters (e.g., IMF and metallicity) of the stellar population model, and even the choice of the model. By measuring the evolution of $M/L$ at other wavelengths than the rest-frame $B$-band, the formation redshift can be established independently, and the range of possible model parameters constrained. Furthermore, the validity of different models can be verified. More specifically, different models predict a different evolution of the $M/L$ in the near infra-red (NIR) relative to the evolution of the optical $M/L$. An advantage of measuring the evolution of the NIR $M/L$ is that the NIR luminosity is less affected by the presence of a low mass young stellar population. Since measuring the evolution of $M/L$ provides a luminosity-weighted age estimate, the evolution of the NIR $M/L$ provides a less biased age estimate. With the arrival of the near Infra-Red Array Camera (IRAC, Fazio et al. 2004) on the Spitzer Space Telescope, studying the rest-frame NIR proper-

---

[1] Based on observations collected at the European Southern Observatory, Chile (169.A-0458).

[2] Based on observations with the *Hubble Space Telescope*, obtained at the Space Telescope Science Institute, which is operated by AURA, Inc., under NASA contract NAS 5-26555

[3] This work is based in part on observations made with the *Spitzer Space Telescope*, which is operated by the Jet Propulsion Laboratory, California Institute of Technology under NASA contract 1407.

[4] Leiden Observatory, P.O.Box 9513, NL-2300 AA, Leiden, The Netherlands

[5] Department of Astronomy, Yale University, P.O. Box 208101, New Haven, CT 06520-8101

[6] Harvard-Smithsonian Center for Astrophysics, 60 Garden Street, Cambridge, MA 02138

[7] Max-Planck-Institut für Astronomie, Königstuhl 17, D-69117 Heidelberg, Germany

[8] University of California Observatories/Lick Observatory, University of California, Santa Cruz, CA 95064

ties of the high-$z$ E/S0 population has become feasible.

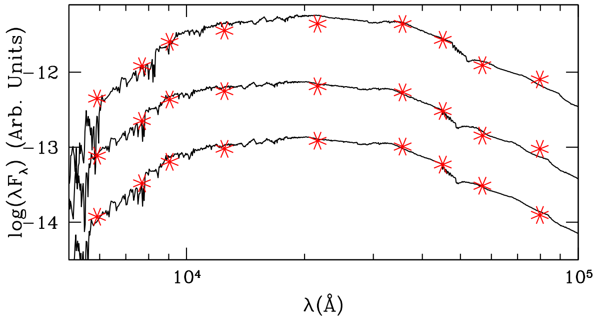

FIG. 1.— SEDs of three $z \sim 1$ E/S0s. The red asterisks are observed fluxes in respectively the ACS ($v$, $i$, $z$), ISAAC ($J$, $K$), and IRAC (3.6, 4.5, 5.8, 8.0) bands. The lines are model spectra from Bruzual-Charlot (a 2 *Gyr*-old, dust-free SSP with solar metallicity and a Salpeter IMF) The photometric SEDs, including the IRAC data points, have plausible shapes of stellar populations of several Gyrs old.

In this *Letter* we combine IRAC imaging with our high-$z$ FP study (van der Wel et al. 2004, 2005), such that the evolution of $M/L$ in the rest-frame $K$-band is measured for the first time. A calibration of galaxy masses derived from NIR luminosities is thus provided.

## 2. IRAC PHOTOMETRY OF E/S0S AT $Z \sim 1$

van der Wel et al. (2005) provide a spectroscopic sample of 29 distant galaxies in the CDFS with accurate velocity dispersions. Spitzer GTO data are available, providing IRAC imaging in four channels (3.6$\mu$, 4.5$\mu$, 5.8$\mu$, and 8.0$\mu$) of a field containing the Chandra Deep Field-South (CDFS). Using the IRAC data we derive the rest-frame NIR photometry of those 20 galaxies in the spectroscopic sample with early-type morphologies and sufficiently high $S/N$ spectra ($S/N \geq 12$ per Å). The average redshift of this sample is $z = 0.94$ and the average mass is $10^{11} M_\odot$. 12 galaxies in this sample are regarded as the 'primary sample': these objects are all at $0.95 < z < 1.15$ and satisfy all selection criteria applied by van der Wel et al. (2005). The other objects, mostly galaxies at $z \sim 0.7$, are referred to as the 'secondary sample'. The IRAC data are sufficiently deep (500s) to obtain high $S/N$ photometry of all galaxies in the sample, certainly in the two shortest wavelength channels.

The IRAC fluxes were measured by matching the point spread functions of all available optical/NIR/IRAC images to the 8.0$\mu$ IRAC image (which has the lowest spatial resolution, $FWHM = 2\farcs3$). $5\farcs0$ diameter aperture fluxes were measured using SExtractor (Bertin & Arnouts 1996) to derive colors. Color gradients are ignored, but because the sizes of the $z \sim 1$ galaxies are much smaller ($r_{eff} \sim 0\farcs4$) than the size of the IRAC PSF this will only have a very small effect. The median formal errors in the IRAC fluxes of the galaxies in the sample are 0.01, 0.01, 0.10 and 0.13 mag for the four channels, respectively. Additionally, the systematic uncertainty in the IRAC zero-points is 0.03 mag. We transformed the observed colors to rest-frame $B-K$ colors using a procedure similar to what is described by van Dokkum & Franx (1996).

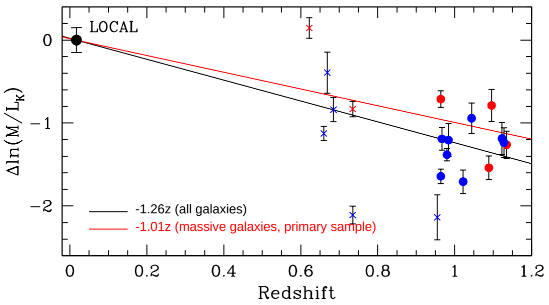

FIG. 2.— $M/L_K$ evolution with redshift of E/S0s in the CDFS. The solid dots are objects in the primary sample, the crosses are the secondary sample. The red symbols are galaxies with high masses ($M > 2 \times 10^{11} M_\odot$), the blue symbols are less massive galaxies. The black data point labeled with 'Local' is derived from local cluster galaxies, but a small difference between field and cluster galaxies is taken into account. The black line indicates the evolution of the entire sample, the red line indicates the evolution of massive galaxies in the primary sample. The evolution of $M/L_K$ of massive galaxies is $\sim 30\%$ slower than the evolution of $M/L_B$ of the same sub-sample.

The typical error in the rest-frame $B-K$ color is 0.06 mag, excluding the systematic error of 0.03 mag. Total luminosities were derived from the structural parameters as obtained from the ACS $z$-band images and the colors are described above.

From the higher resolution $K$-band image we checked whether the IRAC photometry of our sample suffers from confusion. Three of the objects in our sample have close neighbors with such magnitudes that our photometry might be erroneous. However, we do not see a difference between these contaminated objects and the rest of the sample in either color, $M/L$, or any other parameter. In Figure 1 we show the SEDs of three high-redshift E/S0s. As an illustration we overplot a Bruzual & Charlot (2003) model spectrum for a 2 *Gyr*-old stellar population, demonstrating that the observed SEDs have reasonable shapes.

We also measured the colors of a sample of 41 E/S0s in the CDFS at $0.6 < z < 0.8$. These were morphologically selected by eye from the ACS imaging. The redshifts are taken from COMBO-17 (Wolf et al. 2003). We use the average $B-K$ color of this sample to complement the $B-K$ evolution of the galaxies in the FP sample.

## 3. EVOLUTION OF $M/L_K$

If galaxies evolve passively, the offset of high-$z$ galaxies from the local FP is a measure of the difference between the $M/L$ of the distant galaxy and the $M/L$ and their local counterparts (see van Dokkum & Franx 1996). The rate of evolution is a measure of the relative age difference between the local and distant galaxies.

To obtain the $M/L$ evolution in the $K$-band, we compare the NIR properties of the distant galaxies with the local FP in the $K$-band (Pahre et al. 1998), i.e., we need effective radii ($r_{eff}$) and surface brightnesses ($\mu_{eff}$) of the distant galaxies in the rest-frame $K$-band. However, the spatial resolution of IRAC is too low to measure galaxy sizes at $z \sim 1$. Instead we assume that $r_{eff,K} = r_{eff,B}$ and determine the surface brightness at this radius. Although this causes some error in the

FP, previous work has shown that the combination of $r_{eff}$ and $\mu_{eff}$ which enters the FP is very stable against such errors (van Dokkum & Franx 1996). The NIR surface brightness within the optical effective radius is provided by Pahre et al. (1998) for a local sample of cluster galaxies. For the distant sample we compute $\mu_{eff,K}$ from $\mu_{eff,B}$ and $(B-K)_{eff}$, where $(B-K)_{eff}$ is the color inside the effective radius. It is calculated from the total $B-K$ color by correcting for the negative color gradient measured by Peletier et al. (1990). The difference between $B-K$ and $(B-K)_{eff}$ is -0.07 mag.

The local $K$-band FP is based on cluster galaxies, but our sample consists of field galaxies. Faber et al. (1989) have shown that field galaxies have $\sim 5\%$ lower $M/L_B$ than cluster galaxies. Assuming that this difference is caused by either a difference in age or metallicity, this translates into a 2% difference in $M/L_K$, which follows from stellar population models from Bruzual & Charlot (2003). We take this difference into account when comparing the FP at high and low redshifts.

We show the evolution of $M/L_K$ with redshift in Figure 2. It is apparent that $M/L_K$ evolves significantly from $z \sim 1$ to the present. The evolution of the sample is $\Delta \ln(M/L_K) = (-1.26 \pm 0.15)z$, obtained from a least squares linear fit. The primary sample alone evolves at a similar rate: $\Delta \ln(M/L_K) = (-1.18 \pm 0.10)z$. Comparing these numbers to the evolution of $M/L_B$ ($\Delta \ln(M/L_B) = (-1.52 \pm 0.16)z$ and $(-1.46 \pm 0.09)z$, respectively), we see that the evolution in $M/L_K$ is somewhat slower than the evolution in $M/L_B$. The scatter in $\Delta \ln(M/L_K)/z$ is 0.32, which is not much smaller than the scatter in the $B$-band (0.37). This is much larger than can be accounted for by measurement errors, and is most likely caused by an age spread of the stellar populations of the galaxies, as has been demonstrated before (van der Wel et al. 2005). In the $B$-band the measured evolution is strongly mass-dependent (van der Wel et al. 2004; Treu et al. 2005; van der Wel et al. 2005), mostly due to selection effects, but partially due to intrinsic differences between high- and low-mass galaxies (van der Wel et al. 2005). In the $K$-band the difference is much less pronounced, and only marginally significant. The galaxies in the primary sample with masses higher than $M = 2 \times 10^{11} M_\odot$ evolve as $\Delta \ln(M/L_K) = (-1.01 \pm 0.16)z$; galaxies less massive than that as $\Delta \ln(M/L_K) = (-1.27 \pm 0.11)z$. In the $B$-band these numbers are, respectively, $(-1.20 \pm 0.14)z$ and $(-1.60 \pm 0.09)z$. These numbers are consistent with the model prediction that $M/L_K$ is less sensitive than $M/L_B$ to the age of a stellar population and recent star formation.

Concluding, we find that the evolution of $M/L_K$ from $z = 1$ to the present is $\sim 30\%$ slower than the evolution of $M/L_B$. We note that this direct measurement deviates from previous determinations of the evolution of $M/L_K$ that were based on extrapolating observed SEDs (including the $K$-band as the longest wavelength data) to the rest-frame $K$-band at $z \sim 1$ using stellar population models. Such studies found that $M/L_K$ evolves at least twice as slow as $M/L_B$ (see, e.g., Drory et al. 2004). This demonstrates that extrapolating observed $K$-band photometry of high-$z$ galaxies to rest-frame $K$-band $M/L$ is hazardous and strongly model dependent.

## 4. DISCUSSION

Our results allow us to compare the evolution of $M/L_B$ and $M/L_K$ directly with predictions from stellar population models. We compare our results with the predictions of three models: Bruzual & Charlot (2003), Vazdekis et al. (1996), and Maraston (2004) (hereafter, BC03, V96, and M04, respectively). A critical aspect of the models is the method that is used to implement late stellar evolutionary phases. BC03 and V96 compute isochrones up to the early AGB phase, and include an empirical prescription for the thermally pulsating- (TP-) AGB phase. On the contrary, M04 adopt the 'fuel consumption' approach, which allows implementation of short-duration but very luminous evolutionary stages, such as the TP-AGB phases, in an analytical and numerically stable way.

In Figure 3 we compare the evolution from $z = 1$ to the present of $M/L_B$ and $M/L_K$, and the related change in the rest-frame $B-K$ color. The BC03 model with solar metallicity and a Salpeter IMF does not fit the data: the predicted evolution of $M/L_K$ against $M/L_B$ is significantly slower than observed. Before investigating different models and model parameters, we consider several possible explanations for an apparently fast evolution of $M/L_K$ with respect to $M/L_B$ that are unrelated to stellar populations. First, a difference in dust content between local E/S0s and $z \sim 1$ E/S0s could lead to redder colors at $z = 1$ than expected from dust-free models. However, the amount of reddening required to match the BC03 model with solar metallicity and a Salpeter IMF is considerably large for half of the galaxies in our sample ($A_V > 0.5$), and several even require $A_V > 1$. Although the optical spectra show no indication of such high opacities, observations at longer wavelengths with Spitzer can constrain the presence of dust-enshrouded populations which might contribute in the K-band. One might expect to observe irregular morphologies or irregular intensity profiles if the absorption were so high. We note that the galaxies do not show such effects at the ACS resolution. Second, the red colors might be produced by AGN in the $z \sim 1$ sample that are obscured in the optical, but not entirely in the NIR.

Next, we test whether changing parameters within the single-burst BC03 model can improve the consistency between the model and the data. Increasing the metallicity does not change the predictions by much. Changing the star formation history (SFH) does not lead to better fits to the evolution of $M/L_B$ and $M/L_K$, unless models with constant star formation rates or exponentially declining star formation rates with e-folding time scales of several *Gyr* are adopted. These models, however, have very blue colors that do not match the $B-K$ colors of the galaxies in our sample, nor the colors of the local population. Flattening the slope of the IMF (from 1.35 to 0.35) does shift the model curve toward our data points, leading to an acceptable fit.

Finally, we compare our results to other models. As can be seen in Figure 3, the V96 and M04 models with a Salpeter IMF and solar metallicity provide better fits than BC03. Note that the differences between the models with identical parameters are very large; e.g., BC03 predict a correlation between color and $\Delta \ln(M/L)$, whereas M04 does not. We note that the spread of the data

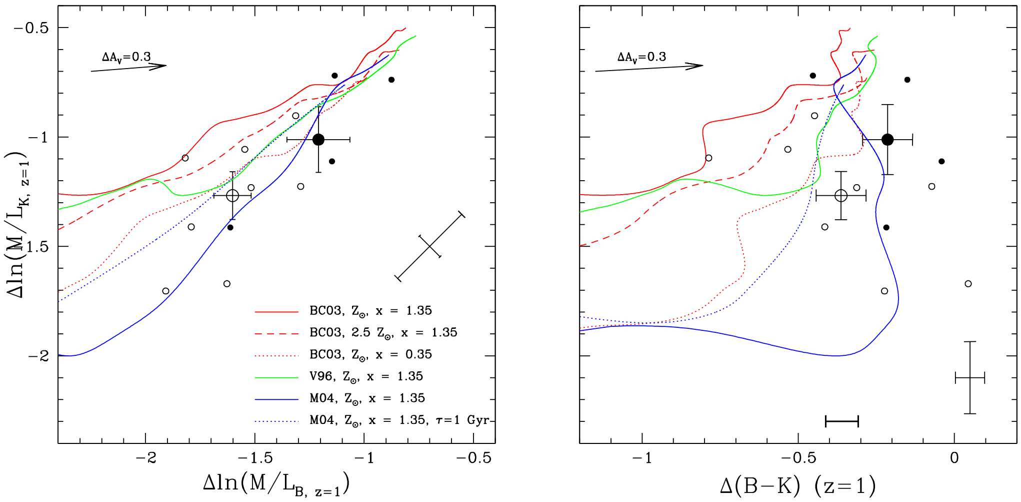

FIG. 3.— Comparison of the $M/L$ evolution in the rest-frame $B$- and $K$-bands and the $B-K$ colors of our $z \sim 1$ E/S0 sample. (Left): the evolution of $M/L_B$ versus the evolution of $M/L_K$, normalized at $z = 1$. The large filled symbol with error bars is the average of the four galaxies in the primary sample with masses larger than $M = 2 \times 10^{11} M_\odot$. The large open symbol with error bars represents the eight less massive galaxies in the primary sample. The smaller symbols are the individual galaxies in the primary sample. The diagonal error bar at the right shows the typical errors in $\Delta \ln M/L_B$ and $\Delta \ln M/L_K$ for the individual data points. The shorter side of the error bar represents the uncertainty in $B-K$. The vector indicates the effect of dust. (Right): the evolution of $B-K$ versus the evolution of $M/L_K$, normalized at $z = 1$. The thick horizontal error bar at the bottom indicates the average $B-K$ evolution extrapolated to $z = 1$ of a sample of 41 E/S0s at $0.6 < z < 0.8$. The model tracks indicate the expected evolution between $z = 1$ and the present, varying the formation redshift along the tracks. The Bruzual-Charlot models with a Salpeter IMF fit badly to the data. A Bruzual-Charlot model with a flat IMF provides a better fit. The Maraston models with a Salpeter IMF provides the best fit. These models have a different treatment of the AGB stars.

points representing the individual galaxies is large, but that there is no clear correlation between $\Delta \ln(M/L_K)$ and $\Delta(B-K)$. Even assuming a flat IMF, the BC03 model cannot reproduce the data points at the bottom right part of Figure 3b. The M04 model does fit to those data points. On the other hand, data points at the upper left of Figure 3b are not fit well by the M04 model. However, all but one of the these data points can be fit with a model with an exponentially declining star formation rate with $\tau = 0 - 1$ Gyr.

We can use the simple single burst models to estimate the average, luminosity-weighted formation redshift of the stellar populations of the galaxies. The formation redshift as estimated from the evolution of $M/L_B$ is $1.6 \leq z_{form} \leq 1.9$ and $1.5 \leq z_{form} \leq 1.9$, using the models from BC03 and M04, respectively, with a Salpeter IMF and solar metallicity. According to the same models, the evolution of $M/L_K$ suggests that $1.2 \leq z_{form} \leq 1.5$ and $1.6 \leq z_{form} \leq 2.0$, respectively. The BC03 model with a flat IMF provides a better fit to our results than the BC03 model with a Salpeter IMF and produces $1.7 \leq z_{form} \leq 2.7$, both from the evolution in the $M/L_B$ and the evolution in $M/L_K$. As can be seen, the constraints on $z_{form}$ are not improved by measuring the evolution of $M/L_K$. This is entirely due to the rather large model uncertainty in the rest-frame $K$-band evolution. Obviously, it is of the greatest relevance to improve our knowledge of both the AGB phase and the dust content of high redshift elliptical galaxies, as dust may mimic some of the results we see.

Finally, we note that E/S0s are thought to be relatively simple systems, with simple SFHs. It is likely that the model uncertainties are even higher for galaxies with a more complex SFH. Irrespective of the causes of the discrepancies between the models and the observations, the results presented here suggest that the rest-frame $K$-band photometry of such galaxies may be difficult to interpret. Further studies of the role of dust and AGN would be valuable. If they do play a role in the photometric bands analyzed here, proper modeling of the colors is more complex than thought before. In the next paper, we will explore full SED fitting, the uncertainties in determining stellar masses, and distinguish between the applicability of different stellar population models.

The authors would like to thank Stijn Wuyts and Ivo Labbé for discussing photometry on IRAC data and the Leidsch Kerkhoven-Bosscha Fonds for financial support. PGvD acknowledges support from NASA LTSA grant NNG04GE12G.

## REFERENCES

Baugh, C. M., Lacey, C. G., Frenk, C. S., Granato, G. L., Silva, L., Bressan, A., Benson, A. J., & Cole, S. 2005, MNRAS, 356, 1191

Bell, E. F., McIntosh, D. H., Katz, N., & Weinberg, M. D. 2003, ApJS, 149, 289

Bell, E. F. et al. 2004, ApJ, 608, 752

Bertin, E., & Arnouts, S. 1996, A&AS, 117, 393

Bruzual, G., & Charlot, S. 2003, MNRAS, 344, 1000
Bundy, K., Ellis, R. S., & Conselice, C. J. 2005, ApJ, in press, astro-ph/0502204
Cappellari, M. et al. 2005, MNRAS, submitted, astro-ph/0505042
Djorgovski, S., & Davis, M. 1987, ApJ, 313, 59
Dressler, A., Lynden-Bell, D., Burstein, D., Davies, R. L., Faber, S. M., Terlevich, R., & Wegner, G. 1987, ApJ, 313, 42
Drory, N., Bender, R., Feulner, G., Hopp, U., Maraston, C., Snigula, J., & Hill, G. J. 2004, ApJ, 608, 742
Faber, S. M., Wegner, G., Burstein, D., Davies, R. L., Dressler, A., Lynden-Bell, D., & Terlevich, R. J. 1989, ApJS, 69, 763
Faber, S. M. et al. 2005, ApJ, submitted, astro-ph/0506044
Fazio, G. G. et al. 2004, ApJS, 154, 10
Gebhardt, K. et al. 2003, ApJ, 597, 239
Holden, B. P. et al. 2005, ApJ, 620, L83
Kauffmann, G., & Charlot, S. 1998, MNRAS, 297, L23
Kelson, D. D., Illingworth, G. D., van Dokkum, P. G., & Franx, M. 2000, ApJ, 531, 184
Maraston, C. 2004, MNRAS, submitted, astro-ph/0410207
Nagashima, M., Lacey, C. G., Okamoto, T., Baugh, C. M., Frenk, C. S., & Cole, S. 2005, MNRAS, submitted, astro-ph/0504618
Pahre, M. A., Djorgovski, S. G., & de Carvalho, R. R. 1998, AJ, 116, 1591
Peletier, R. F., Valentijn, E. A., & Jameson, R. F. 1990, A&A, 233, 62
Shapley, A. E. et al. 2005, ApJ, accepted, astro-ph/0503485
Treu, T., Ellis, R. S., Liao, T. X., & van Dokkum, P. G. 2005, ApJ, in press, astro-ph/0502028
Treu, T., Stiavelli, M., Bertin, G., Casertano, S., & Møller, P. 2001, MNRAS, 326, 237
Treu, T., Stiavelli, M., Casertano, S., Møller, P., & Bertin, G. 2002, ApJ, 564, L13
van der Wel, A., Franx, M., van Dokkum, P. G., & Rix, H.-W. 2004, ApJ, 601, L5
van der Wel, A., Franx, M., van Dokkum, P. G., Rix, H.-W., Illingworth, G., & Rosati, P. 2005, ApJ, 631, 145
van Dokkum, P. G., & Ellis, R. S. 2003, ApJ, 592, L53
van Dokkum, P. G., & Franx, M. 1996, MNRAS, 281, 985
van Dokkum, P. G., Franx, M., Kelson, D. D., & Illingworth, G. D. 1998, ApJ, 504, L17
—. 2001, ApJ, 553, L39
van Dokkum, P. G., & Stanford, S. A. 2003, ApJ, 585, 78
Vazdekis, A., Casuso, E., Peletier, R. F., & Beckman, J. E. 1996, ApJS, 106, 307
Wolf, C., Meisenheimer, K., Rix, H.-W., Borch, A., Dye, S., & Kleinheinrich, M. 2003, A&A, 401, 73
Wuyts, S., van Dokkum, P. G., Kelson, D. D., Franx, M., & Illingworth, G. D. 2004, ApJ, 605, 677